On the Synthesis of Spatial Cycloidal Gears

Giorgio Figliolini [1], Hellmuth Stachel [2], Jorge Angeles [3]

[1] *DiMSAT, University of Cassino*
E-mail: figliolini@unicas.it

[2] *Institute of Discrete Mathematics and Geometry, University of Technology, Vienna, Austria*
E-mail: stachel@dmg.tuwien.ac.at

[3] *Department of Mechanical Engineering & CIM, McGill University, Montreal, Canada*
E-mail: angeles@cim.mcgill.ca

SUMMARY. The subject of this paper is the synthesis of spatial cycloidal gears, based on Disteli's work, which was published at the turn of the 20th century. In particular, the properties of the cylindroid or Plücker's conoid for the relative motion between a pair of skew gears are analyzed in order to extend Reuleaux's principle from the planar and spherical cases to the spatial case with the aim of synthesizing a pair of conjugate cycloidal teeth.

1 INTRODUCTION

Skew gears allow the transmission of motion between gears with skew axes at either constant or a variable transmission ratio by means of a pair of axially symmetric or, correspondingly, non-symmetric pitch surfaces. Consequently, gears with parallel or intersecting axes become particular cases. Thus, the formulation of a general algorithm for the synthesis of gears with skew axes is of great interest not only from a research viewpoint but also by virtue of its industrial applications. This formulation is quite a challenging.

In the literature, some interesting and useful results have been obtained along these lines, as reported in [1-4]. However, the modeling of gears with skew axes and involute teeth is still an open question, as it has become apparent, for instance, that the meaning of involute teeth in the case of spatial gears has not been elucidated. Indeed, the extension of the concept of evolute-involute from the planar and spherical cases to the spatial case is not straightforward. Consequently, the properties of the involute teeth cannot be readily extended to gears with skew axes. For example, Phillips [3] could define involute teeth in gears with skew axes upon assuming that the contact point is located, at any instant, along a line that is skew with respect to the gear axes. This result was proven geometrically and with the aid of useful animations by Stachel [4].

Therefore, our research is aimed at formulating a general algorithm for the synthesis of gears with skew axes by applying a fundamental procedure: 1) the hyperboloid pitch surfaces that are derived from the relative layout between the two skew axes and the constant transmission ratio are first obtained; 2) the Plücker conoid determined by the relative motion of the two meshing gears is then synthesized as the locus of the instant screw axis; 3) with the aid of the cylindroid, we introduce an auxiliary surface (AS); and 4) as the AS moves while maintaining line contact with the two hyperboloid pitch surfaces, a pair of conjugate flanks is synthesized. In particular, the AS is a helical surface in the case of skew cycloidal gears.

This paper focuses on the synthesis of spatial cycloidal gears based on Disteli's work, which was published at the turn of the 20th century [5-6]. In particular, the properties of the cylindroid or

Plücker's conoid for the relative motion between a pair of skew gears are analyzed in order to extend Reuleaux's principle from the planar and spherical cases, as reported in [7-9], to the spatial case with the aim of synthesizing a pair of conjugate cycloidal teeth.

Ongoing work related has been published by the authors [10-12]. In fact, the synthesis of the pitch surfaces of any pair of external and internal skew gears, using dual algebra and the principle of transference, was proposed in [10]. Hyperboloid pitch surfaces of the driving and driven gears were synthesized, along with the helicoidal pitch surfaces of their rack.

Later, the Ball-Disteli diagram was revisited [11] using dual algebra. In fact, this diagram can be very useful for several applications regarding the analysis and design of gears with skew axes, because it allows the visualization of the relations among motion variables and geometric parameters regarding the relative motion between the two meshing gears. More recently, the authors extended the results reported by Martin Disteli at the turn of the 20th century concerning the general synthesis of gears with skew axes and cycloidal teeth by means of the dualization of the tooth profiles of spherical cycloidal gears [12]. In this way, conjugate tooth flanks, characterized by having the contact points located on a straight line, could be obtained.

The novelty of this paper lies in the analysis of the relative motion between a pair of skew gears by means of Plücker's conoid, in order to extend Reuleaux's principle from the planar and spherical cases to the spatial case. In fact, the problem is to find the right auxiliary surface, in order to obtain spatial cycloidal and involute gears. In particular, this paper regards the synthesis of spatial cycloidal gears by resorting to Disteli's work.

2   RELATIVE SCREW-MOTION AND HYPERBOLOID PITCH SURFACES

The relative screw-motion between the driving and driven gears along with the hyperboloid pitch surfaces and their helicoidal rack were analyzed in [10] through the application of dual algebra and the principle of transference. Some results are recalled below.

With reference to Fig.1a, the driving gear 2 is assumed to be rotating about the I_2 axis, which is coincident with the Z-axis of the fixed frame $\mathcal{F}(\,O\,X\,Y\,Z\,)$, while the position of the I_3 axis of the driven gear 3 is given by angle α_1 and distance a_1 along the positive X-axis. The Instant Screw Axis I_{32}, ISA for brevity, of the relative motion can be determined by means of the Aronhold-Kennedy theorem in three dimensions. In fact, all three axes, I_2, I_3 and I_{32}, share the X-axis as their common perpendicular, while angle ϑ_2 and the coordinate b_2 determine the I_{32}-axis.
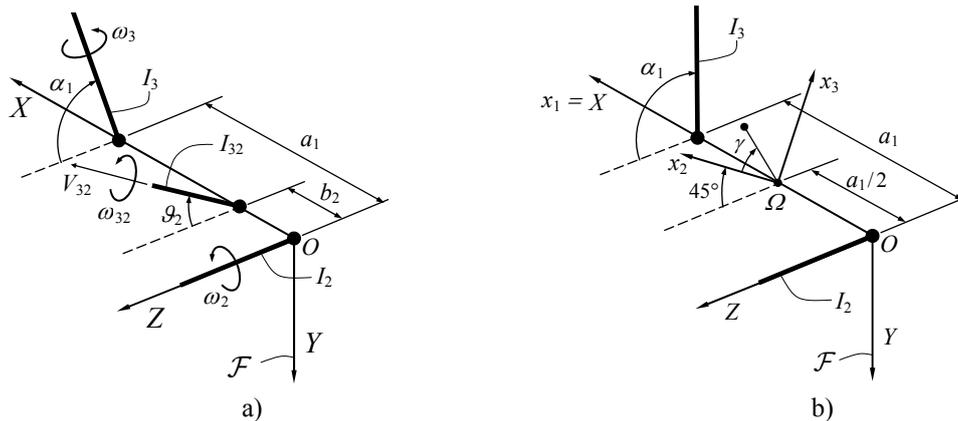

Figure 1: Reference frames: a) relative screw motion; b) Plücker's conoid.

Referring to the formulation proposed in [10], the relative angular and sliding velocities ω_{32} and V_{32}, respectively, can be expressed in the form

$$\omega_{32} = \pm\omega_3 \sqrt{1 - 2\,k\cos\alpha_1 + k^2} \qquad (1)$$

and

$$V_{32} = \frac{k\,\omega_3\,a_1\sin\alpha_1}{\pm\sqrt{1 - 2\,k\cos\alpha_1 + k^2}}, \qquad (2)$$

where $k = \omega_2/\omega_3$ is the transmission ratio between the pair of skew gears, which is negative for external gears and positive for internal gears.

Likewise, the position of the ISA in the fixed frame $\mathcal{F}(O\,X\,Y\,Z)$ is given through the oriented angle ϑ_2 and the distance b_2, which can be expressed as

$$\tan\vartheta_2 = \frac{\sin\alpha_1}{\cos\alpha_1 - k} \qquad (3)$$

and

$$b_2 = \frac{1 - k\cos\alpha_1}{1 - 2\,k\cos\alpha_1 + k^2}\,a_1. \qquad (4)$$

The hyperboloid pitch surface of the driving gear 2 can be expressed in the form

$$\mathbf{r}_2(\psi,\lambda) = b_2 \begin{bmatrix} \cos\psi \\ -\sin\psi \\ 0 \end{bmatrix} + \lambda \begin{bmatrix} -\sin\psi\,\sin\vartheta_2 \\ -\cos\psi\,\sin\vartheta_2 \\ \cos\vartheta_2 \end{bmatrix}, \qquad \lambda \in \mathbb{R} \qquad (5)$$

where $\mathbf{r}_2$ is the position vector of a point of the line generating the pitch surface.

Likewise, the hyperboloid pitch surface of the driven gear 3 is given by

$$\mathbf{r}_3(\varphi,\lambda) = (b_2 - a_1) \begin{bmatrix} \cos\varphi \\ \sin\varphi\,\cos\alpha_1 \\ -\sin\varphi\,\sin\alpha_1 \end{bmatrix} - \lambda \begin{bmatrix} \sin\varphi\,\sin(\vartheta_2 - \alpha_1) \\ \cos\varphi\,\sin(\vartheta_2 - \alpha_1)\cos\alpha_1 - \cos(\vartheta_2 - \alpha_1)\sin\alpha_1 \\ \cos\varphi\,\sin(\vartheta_2 - \alpha_1)\sin\alpha_1 + \cos(\vartheta_2 - \alpha_1)\cos\alpha_1 \end{bmatrix} + \begin{bmatrix} a_1 \\ 0 \\ 0 \end{bmatrix} \qquad (6)$$

because of the translation a_1 along the X-axis and the rotation α_1 with respect to the Z-axis.

Therefore, Eqs. (1) and (2) allow the analysis of the relative kinematics between the pair of skew gears, which is characterized by a screw-motion with minimum sliding velocity V_{32} along the ISA, while Eqs. (3) to (6) give geometric results, because they allow the representation, in the fixed frame $\mathcal{F}(O\,X\,Y\,Z)$, of the hyperboloid pitch surfaces of the driving and driven gears, 2 and 3, respectively.

More details regarding the formulation of the pitch surface of their rack can be found in [10], along with the complete algorithm for the synthesis of the pitch surfaces of any pair of external and internal skew gears, which was implemented in Matlab.

3 PLÜCKER'S CONOID

When the relative position of the skew axes of rotation I_2 and I_3 is given through the distance a_1 and angle α_1, the position of the instantaneous screw-axis I_{32} for the relative motion between the skew gears, which is given by distance b_2 and angle ϑ_2, changes according to the variation of the transmission ratio k in the range ($+\infty$, $-\infty$). During the variation of its position, I_{32} remains perpendicular to the common normal of I_2 and I_3, according to the Aronhold-Kennedy Theorem in three-dimensions, and traces a ruled surface that is named the Plücker conoid. In other words, even if k changes in the range ($+\infty$, $-\infty$), the locus described by the instantaneous screw-axis I_{32} is represented by a finite ruled surface.

In fact, solving Eq. (4) for the transmission ratio k, one obtains a second-order algebraic equation, whose roots are

$$ k = \frac{1}{2b_2}\left[(2b_2 - a_1)\cos\alpha_1 \pm \sqrt{(a_1 - 2b_2)^2 \cos^2\alpha_1 + 4b_2(a_1 - b_2)} \right]. \qquad (7) $$

Thus, the limits of the Plücker conoid can be determined by the vanishing of the discriminant of Eq. (7), which leads to the two extreme positions of I_{32}, namely,

$$ b_2 = \frac{a_1}{2}\left[1 \pm \frac{1}{\sin\alpha_1} \right], \qquad (8) $$

which are the positions of the two torsal generators of the Plücker conoid.

In particular, referring to Fig. 2a, when $\alpha_1 = 0°$, which means cylindrical gears, one obtains from Eq. (8) that b_2 can take on any value in the range ($+\infty$, $-\infty$). In this case the Plücker conoid, becomes unbounded, namely, a plane containing both axes of rotation, I_2 and I_3. When $\alpha_1 = 90°$, one obtains from Eq. (8) that b_2 can vary in the range [0 , a_1], as shown in Fig. 2b.
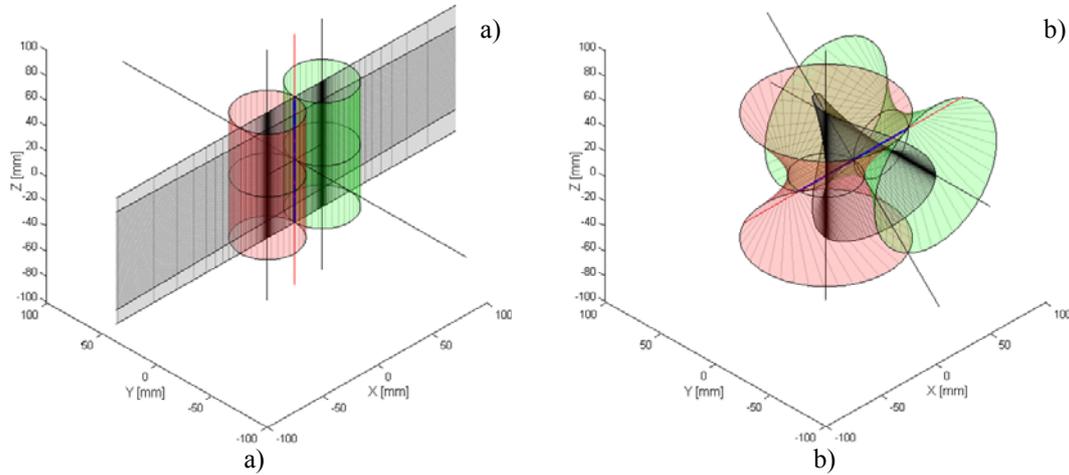

Figure 2: Hyperboloid pitch surfaces for $k = -1$ and Plücker's conoid: a) $\alpha_1 = 0°$ and $a_1 = 50$ mm with $b_2 \in$ ($+\infty$, $-\infty$); b) $\alpha_1 = 90°$ and $a_1 = 50$ mm with $b_2 \in$ [0 , a_1].

The equation of the Plücker conoid in $\mathcal{F}(O\,X\,Y\,Z)$ can be expressed in the form

$$\mathbf{r}(\vartheta_2, b_2, \lambda) = \begin{bmatrix} b_2 \\ 0 \\ 0 \end{bmatrix} + \lambda \begin{bmatrix} 0 \\ -\sin\vartheta_2 \\ \cos\vartheta_2 \end{bmatrix}, \tag{9}$$

where the limits of λ can be chosen arbitrarily, because they define only the extension of the Plücker conoid, while the parameters ϑ_2 and b_2 are obtained from Eqs. (3) and (4), respectively, when the transmission ratio k varies in the range $(+\infty, -\infty)$. For instance, the limits of λ can be chosen equal to the width of the pitch surfaces, as shown in Fig. 2.

Specific kinematic and geometric properties of the Plücker conoid are useful for understanding the basic concepts related to the synthesis of spatial gears, as described below.

There must exist two special screws of zero pitch on the Plücker conoid, since the pitch varies continuously and periodically as the ratio k increases from $-\infty$ to $+\infty$. Since any two screws on a given Plücker's conoid define the same cubic surface, it is convenient to discuss the Plücker conoid in terms of its two screws of zero pitch. In fact, in the case of spatial gears, these two screws are the two axes of rotation I_2 and I_3. This property can be demonstrated by expressing the pitch $p_{32} = V_{32} / \omega_{32}$ of the screw with axis I_{32} as

$$p_{32} = \frac{k\, a_1 \sin\alpha_1}{1 - 2\,k\cos\alpha_1 + k^2}, \tag{10}$$

which can be done by recalling Eqs. (1) and (2). Thus, the two zero-pitch screws are obtained for $k = 0$ and $k \to \pm\infty$, which give I_3 and I_2, respectively, from Eqs. (3) and (4).

Then, referring to what is reported in [11] about the Ball-Disteli diagram, a plane that contains one of the screws of the Plücker conoid intersects it along a cubic curve that decomposes into a conic and the line of the screw itself. This conic is an ellipse because the general Plücker conoid is bounded by two parallel planes and, hence, the conic must be finite everywhere except when the plane is perpendicular to the nodal line or common normal between I_2 and I_3, in which case the intersection degenerates into two lines or generators along with the line at infinity of the plane itself. Referring to Fig. 1b, this property can be demonstrated by expressing the Plücker conoid in the fixed frame (Ω, x_1, x_2, x_3) as

$$x_1 = a_1 \frac{x_3\, x_2}{x_3^2 + x_2^2} \tag{11}$$

$$x_2 = \pm\sqrt{a_1^2 - x_3^2} \tag{12}$$

where Eq. (11) represents the cubic surface of the Plücker conoid, while Eq. (12) represents a cylinder having its axis coinciding with the x_1 - axis. The intersection between these surfaces gives the skew curve of Fig. 3.

Moreover, the intersection of the Plücker conoid with a plane that contains one of its screws can be obtained as the intersection of the conoid with a cylinder of diameter a_1, which passes through the nodal line (x_1-axis) of the Plücker conoid. This cylinder can be expressed as

$$x_3^2 + x_2^2 - x_3\, a_1 \sin\gamma - x_2\, a_1 \cos\gamma = 0, \tag{13}$$

where γ is an oriented angle with respect to the x_2 - axis, which gives the position of the cylinder of Eq. (13) in the fixed frame (Ω, x_1, x_2, x_3) of Fig. 1b. Figure 3 shows a rendering of the results.
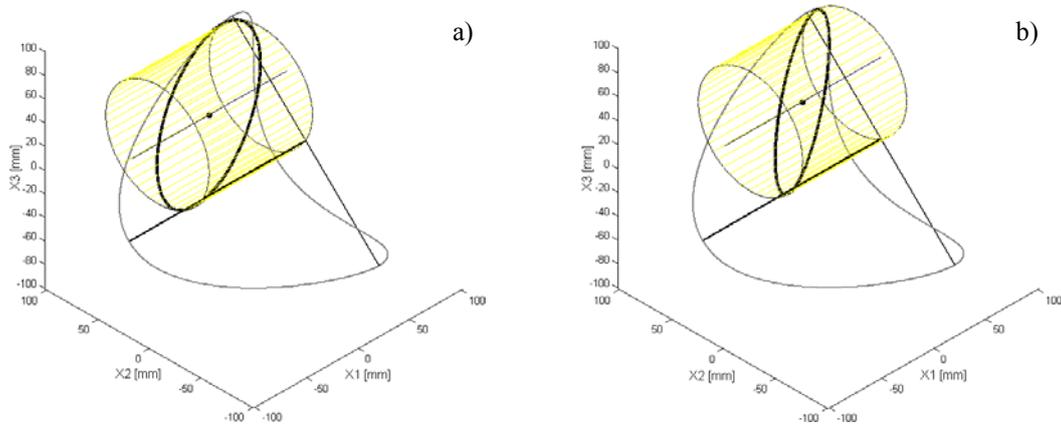
Figure 3: Skew ellipse as intersection of the Plücker conoid with a circular cylinder of diameter $a_1 = 100$ mm, which passes through the nodal line of the cubic surface: a) $\gamma = 30°$; b) $\gamma = 60°$.

4   REULEAUX'S PRINCIPLE

Reuleaux's principle in the planar case, which sometimes is attributed to Camus [13], states that "If an auxiliary curve is rolling on the pitch circles of circular gears, any point attached to this curve traces conjugate profiles". In particular, when the auxiliary curve is a circle or a logarithmic spiral, cycloidal and involute gears are obtained, respectively, as reported in [7].

Referring to Fig. 4a, when two circles ε_1 and ε_2 with equal radii m are chosen as auxiliary curves, their rolling on each pitch circle $\mathcal{P}$ generates a pair of conjugate tooth profiles, which are cycloidal curves $\mathcal{C}$ in this particular case. In general, instead of a point, a smooth curve can be given as attached to the auxiliary curve. Consequently, during the pure rolling motion of the auxiliary curve on the pitch circles, two families of curves are obtained, their envelopes giving two conjugate profiles. In fact, referring to Fig. 4b, each involute tooth profile $\mathcal{I}$ can be obtained as envelope of the line η, which is attached to the line ε that is tangent to each pitch circle $\mathcal{P}$. Of course, the same involute tooth profile can be also obtained by rolling without sliding the line $\mathcal{N}$, which is normal to $\mathcal{I}$ and η, and passes through the instant center of rotation I, on the base circle $\mathcal{B}$ that is also the evolute of $\mathcal{I}$. Point T is the center of curvature of $\mathcal{I}$ at the contact point P, r_b and r_p are the radii of the base and pitch circles, respectively, and angle ϕ is the pressure angle.
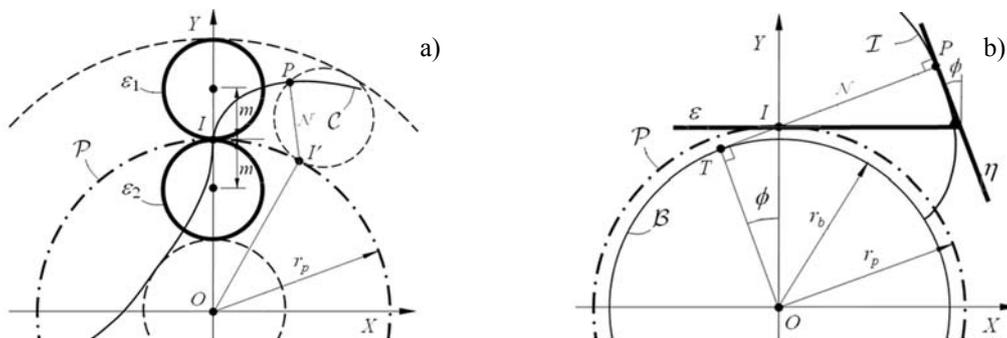

Figure 4: Application of the Reuleaux principle: a) cycloidal gears; b) involute gears.

Reuleaux's principle is also valid in the spherical case and, thus, it can be applied to the synthesis of bevel gears with cycloidal and involute tooth profiles.

Nevertheless, the generalization of Reuleaux's principle to the spatial case and, in particular, to the synthesis of involute conjugate teeth of skew gears, is not available. Phillips proposed in his book [3] a procedure for the synthesis of "involute" spatial gearing by using a different approach, which was geometrically validated by Stachel [4], but this procedure is not based on Reuleaux's principle; even the meaning of "involute" is lost under Phillips' hypothesis.

In particular, a suitable algorithm for the synthesis of cycloidal skew gears, simpler than their involute counterparts, is proposed here, with first results reported in the accompanying figures, where the hyperboloid pitch surfaces of a pair of skew gears are shown, along with their Plücker conoid. Moreover, particular attention is given to the helicoids, which are tangent to both hyperboloids along the Instant Screw Axis, because these surfaces represent the auxiliary surfaces for generating a pair of conjugate cycloidal teeth.

5 SYNTHESIS OF SPATIAL CYCLOIDAL GEARS

According to Reuleaux's principle and referring to Fig. 5, both auxiliary surfaces for the synthesis of the conjugate tooth flanks of spatial cycloidal gears with line contact, can be determined by defining the positions of their axes I_5 and I_6 on the Plücker conoid.

Thus, taking into account the common rule to assume equal radii for both circles ε_1 and ε_2 of Fig. 4a for the synthesis of planar cycloidal gears, even in the spatial case, the same distance m from the instant screw axis I_{32} and along their common normal (X - axis) can be chosen, in order to determine both auxiliary surfaces AS_5 and AS_6, which take the place of the circles ε_1 and ε_2 of the planar case, respectively.

The positions on the Plücker conoid of both instant screw axes I_5 and I_6 of the auxiliary surfaces AS_5 and AS_6, respectively, can be determined by assuming a suitable value of the transmission ratio k_5 and calculating both distance b_5 and angle ϑ_5 from the Eqs. (3) and (4), respectively, as shown in the sketch of Fig. 5a and numerical example of Fig. 5b.
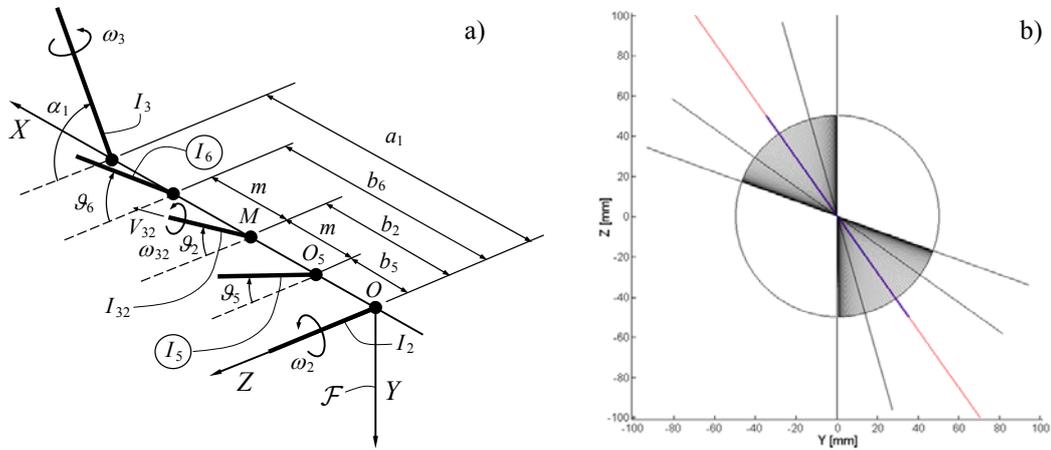

Figure 5: Positions of the axes I_2, I_3, I_{32}, I_5 and I_6 in the fixed frame $\mathcal{F}(O X Y Z)$: a) kinematic sketch; b) example for $\alpha_1 = 70°$, $a_1 = 50$ mm, $k = -1$, $b_2 = 25$ mm, $\vartheta_2 = 35°$, $k_5 = -3$, $b_5 = 8,4054$ mm, $\vartheta_5 = 15,7047°$, $m = 16,5946$ mm, $b_6 = 41,5946$, $k_6 = -0,3333$, $\vartheta_6 = 54,2953°$.

In fact, for example, when $\alpha_1 = 70°$, $a_1 = 50$ mm and $k = -1$, the position of the ISA is determined from Eqs. (3) and (4), which give $\vartheta_2 = 35°$ and $b_2 = 25$ mm. Moreover, assuming a transmission ratio $k_5 = -3$, the position of the instant screw axis I_5 of AS$_5$ is still obtained through Eqs. (3) and (4), which give $\vartheta_5 = 15,7047°$ and $b_5 = 8,4054$ mm, respectively.

The value of m is obtained from the difference between b_2 and b_5, which allows the determination of b_6 as the sum of b_2 and m by giving in this case $m = 16,5946$ mm and $b_6 = 41,5946$ mm, respectively. Finally, the transmission ratio k_6 can be obtained from Eq. (7) by referring to b_6 instead of b_2, which allows the determination of ϑ_6 from Eq. (3) by referring to k_6 instead of k. For the proposed example, one obtains $k_6 = -0,3333$ and $\vartheta_6 = 54,2953°$, respectively. Therefore, I_5 and I_6 are the screw axes of the auxiliary surfaces AS$_5$ and AS$_6$, respectively, which can be determined by rotating and translating the ISA across and along these axes respectively in order to generate two helicoids, as AS of spatial cycloidal gears.

However, this rigid motion of the ISA requires a spatial kinematic analysis that is aimed at determining the absolute angular velocities ω_5 and ω_6 and the sliding velocities V_5 and V_6 of both screws with axes I_5 and I_6. This can be done by imposing that both axes I_{52} and I_{62} for the relative motion of AS$_5$ and AS$_6$ with respect to the driving gear 2 are coincident with the ISA [12, Theorem 3]. Thus, taking into account that $\boldsymbol{\omega}_5$ and $\boldsymbol{\omega}_2$ are the angular velocity vectors of the AS$_5$ and the driving gear 2, respectively, their relative angular velocity vector $\boldsymbol{\omega}_{52}$ is obtained by

$$\omega_{52}\begin{bmatrix} 0 \\ -\sin\vartheta_2 \\ \cos\vartheta_2 \end{bmatrix} = \omega_5\begin{bmatrix} 0 \\ -\sin\vartheta_5 \\ \cos\vartheta_5 \end{bmatrix} - \omega_2\begin{bmatrix} 0 \\ 0 \\ 1 \end{bmatrix}, \tag{14}$$

which gives the expression of the magnitude ω_5 of $\boldsymbol{\omega}_5$ in the form

$$\omega_5 = \omega_2\frac{\sin\vartheta_2}{\sin(\vartheta_2 - \vartheta_5)}. \tag{15}$$

Likewise, taking into account that $\mathbf{V}_5$ is the velocity vector of the AS$_5$ along its I_5-axis, while $\mathbf{b} = b_2\,\mathbf{i}$ and $\mathbf{m} = m\,\mathbf{i}$ are the position vectors of point M with respect to O and O_5, along the X-axis of Fig. 5a, their relative velocity vector $\mathbf{V}_{52}$ is obtained by

$$V_{52}\begin{bmatrix} 0 \\ \sin\vartheta_2 \\ -\cos\vartheta_2 \end{bmatrix} = \left(V_5\begin{bmatrix} 0 \\ \sin\vartheta_5 \\ -\cos\vartheta_5 \end{bmatrix} + \boldsymbol{\omega}_5\times\mathbf{m} \right) - \boldsymbol{\omega}_2\times\mathbf{b}, \tag{16}$$

which gives the expression of the magnitude V_5 of $\mathbf{V}_5$ in the form

$$V_5 = \frac{\omega_2\,b_2\cos\vartheta_2 - \omega_5\,m\cos(\vartheta_2 - \vartheta_5)}{\sin(\vartheta_2 - \vartheta_5)}. \tag{17}$$

Therefore, the knowledge of both angular and sliding velocities ω_5 and V_5, which pertain to the screw axis I_5, allow the determination of the helicoidal AS$_5$ that is tangent to the two pitch surfaces of the gears 2 and 3 along the ISA. Similarly, both angular and sliding velocities ω_6 and V_6 allowed the determination of the helicoidal AS$_6$. Examples of Figs. 6 to 13 show the AS$_5$ and AS$_6$, the Plücker conoid and the hyperboloid pitch surfaces, along with their helicoid rack.
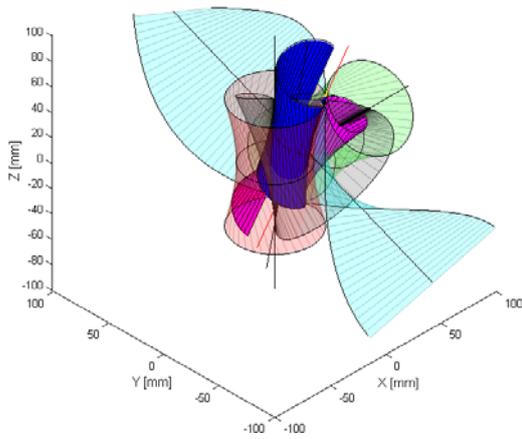
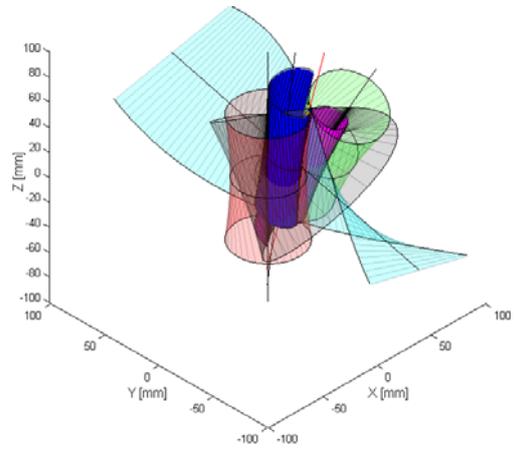Fig. 6: $k = -1$, $\alpha_1 = 45°$, $a_1 = 50$ mm, $k_5 = -3$

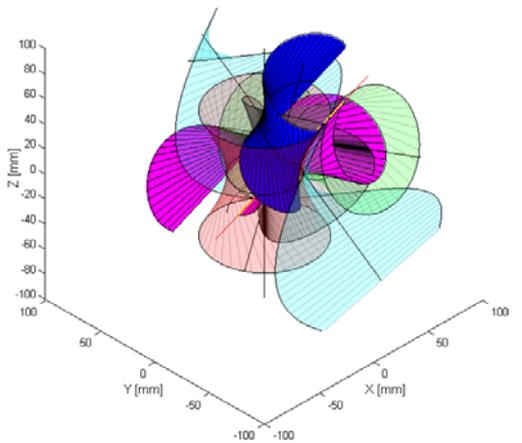Fig. 7: $k = -1$, $\alpha_1 = 30°$, $a_1 = 50$ mm, $k_5 = -3$

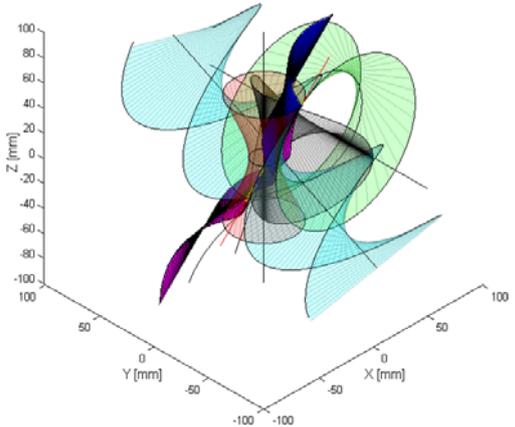Fig. 8: : $k = -1$, $\alpha_1 = 70°$, $a_1 = 50$ mm, $k_5 = -3$

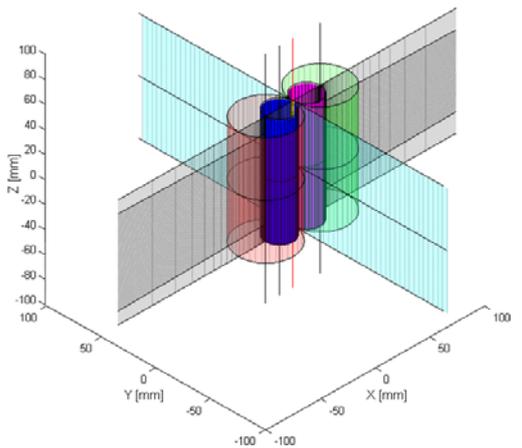Fig. 9: $k = -2$, $\alpha_1 = 90°$, $a_1 = 50$ mm, $k_5 = -3$

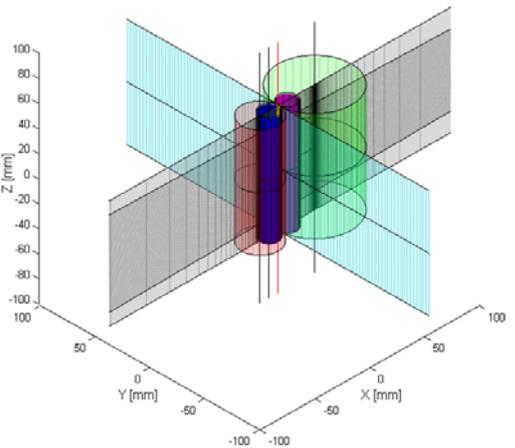Fig. 10: $k = -1$, $\alpha_1 = 0°$, $a_1 = 50$ mm, $k_5 = -3$

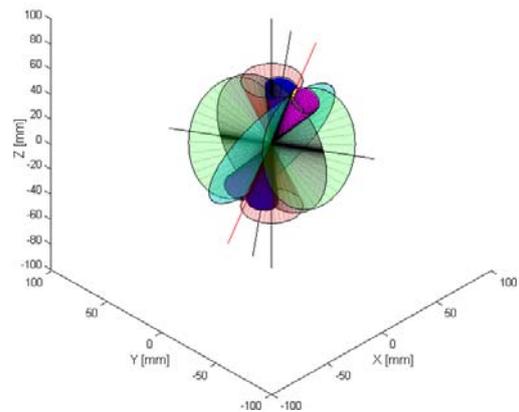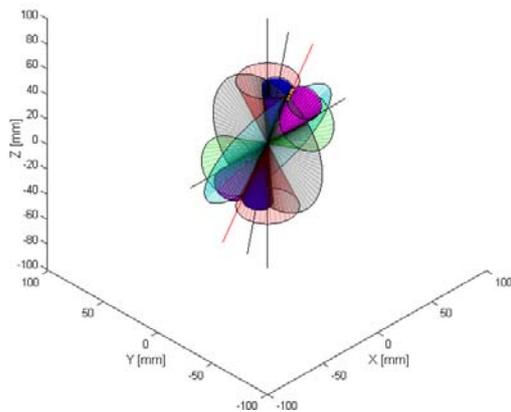Fig. 11: $k = -2$, $\alpha_1 = 0°$, $a_1 = 50$ mm, $k_5 = -5$

Fig. 12: $k = -1$, $\alpha_1 = 45°$, $a_1 = 0$ mm, $k_5 = -3$ Fig. 13: $k = -2$, $\alpha_1 = 70°$, $a_1 = 0$ mm, $k_5 = -5$

6 CONCLUSIONS

Franz Reulaux's principle was extended to the case of skew cycloidal gears. This approach could be extended further, to the case of involute skew gears, but the extension is challenging because each tooth flank should be obtained as the envelope of a given surface attached to the auxiliary surface.

References
[1] Litvin F.L. and Fuentes A., Gear Geometry and Applied Theory, Cambridge University Press, Cambridge, 2004.
[2] Dooner D.B. and Seireg A.A., The Kinematic Geometry of Gearing: A Concurrent Engineering Approach, John Wiley & Sons, Inc., New York, 1995.
[3] Phillips J., General Spatial Involute Gearing, Springer-Verlag, Berlin, 2003.
[4] Stachel H., On Jack Phillips Spatial Involute Gearing, 11th International Conference on Geometry and Graphics, Guangzhou (China), 2004, pp. 43-48.
[5] Disteli M., Über instantane Schraubengeschwindigkeiten und die Verzahnung der Hyperboloidräder, Z. Math. Phys, 1904, **51**, pp.51-88.
[6] Disteli M., Über die Verzahnung der Hyperboloidräder mit geradlinigem Eingriff, Z. Math. Phys, 1911, **59**, pp.244-298.
[7] Reuleaux F., The Kinematics of Machinery, English version by Alexander B. W. Kennedy, Dover, New-York, 1963.
[8] Ghigliazza R., Lucifredi A. and Michelini R., Meccanica Applicata alle Macchine, Microlito, Genova, 1974.
[9] Ferrari C. and Romiti A., Meccanica Applicata alle Macchine, UTET, Torino, 1966.
[10] Figliolini G. and Angeles J., The Synthesis of the Pitch Surfaces of Internal and External Skew-Gears and their Racks, ASME J. of Mechanical Design, 2006, **128** (4), pp.794-802.
[11] Figliolini G., Stachel H. and Angeles J., A New Look at the Ball-Disteli Diagram and its Relevance to Spatial Gearing, Mechanism and Machine Theory, **42**, 2007, pp.1362-1375.
[12] Figliolini G., Stachel H. and Angeles J., The Computational Fundamentals of Spatial Cycloidal Gearing, Proc. of the 5th International Workshop on Computational Kinematics, Springer, Kecskeméthy A. and Müller A. (Eds.), Springer-Verlag, Berlin, 2009, pp.375-384.
[13] Camus, Ch.-E., Éléments de mechanìque statique, Durand Publisher, Paris, 1759.